Electronic Supplementary Material (ESI) for Energy & Environmental Science.
This journal is © The Royal Society of Chemistry 2018

Electronic supplementary information for:

Boosting oxygen reduction catalysis with abundant copper single atom active sites

Feng Li[a], Gao-Feng Han[a], Hyuk-Jun Noh[a], Seok-Jin Kim[a], Yalin Lu[bcd], Hu Young Jeong*[e], Zhengping Fu*[bc], Jong-Beom Baek*[a]

[a] School of Energy and Chemical Engineering/Center for Dimension-Controllable Organic Frameworks, Ulsan National Institute of Science and Technology (UNIST), 50 UNIST, Ulsan 44919, South Korea.

[b] CAS Key Laboratory of Materials for Energy Conversion, Department of Materials Science and Engineering, University of Science and Technology of China (USTC), Hefei 230026, P. R. China.

[c] Synergetic Innovation Center of Quantum Information and Quantum Physics and Hefei National Laboratory for Physical Sciences at Microscale, University of Science and Technology of China (USTC), Hefei 230026, P. R. China.

[d] National Synchrotron Radiation Laboratory, University of Science and Technology of China (USTC), Hefei 230026, P. R. China.

[e] UNIST Central Research Facilities, Ulsan National Institute of Science and Technology (UNIST), 50 UNIST, Ulsan 44919, South Korea.

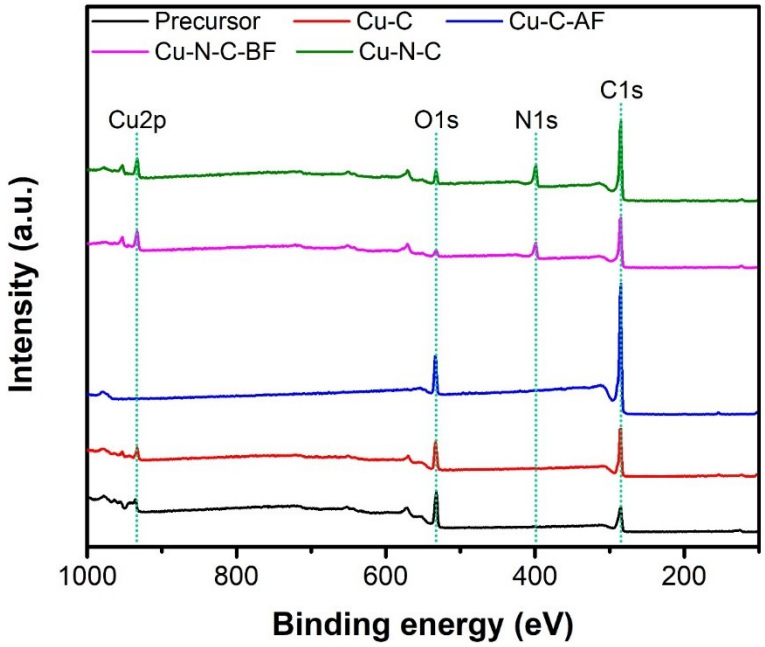

Figure S1. XPS survey spectra of the precursor, Cu-C, Cu-C-AF, Cu-N-C-BF and Cu-N-C, respectively.

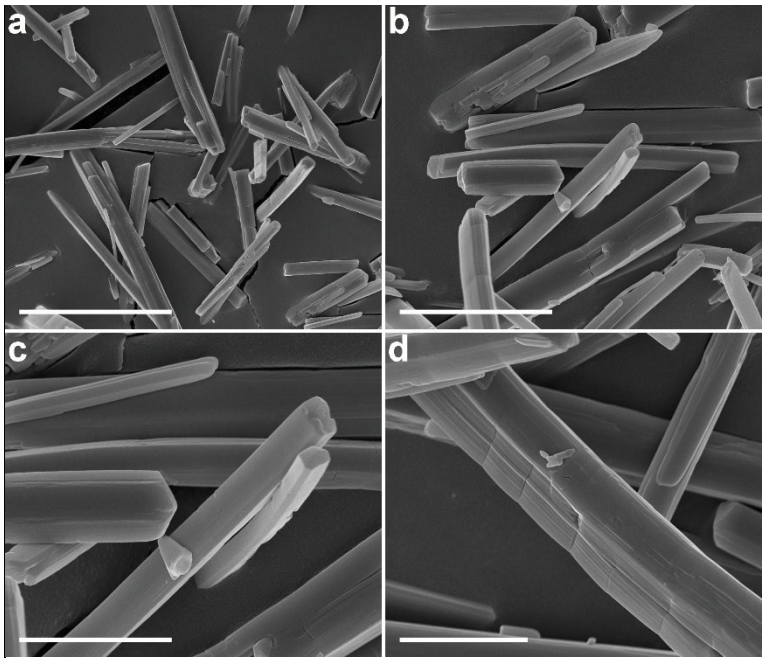

Figure S2. SEM images of the precursor of Cu-N-C at different magnification. Scale bars: (**a**) 20 μm; (**b**) 10 μm; (**c**, **d**) 5 μm.

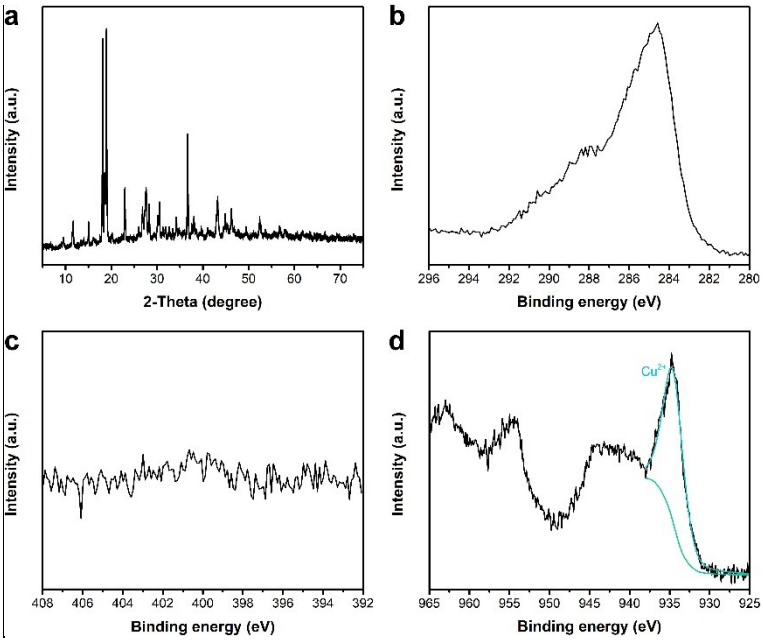

Figure S3. XRD pattern and XPS survey spectra of the precursor of Cu-N-C: (**a**) XRD pattern, (**b**) C 1s, (**c**) N 1s, (**d**) Cu 2p.

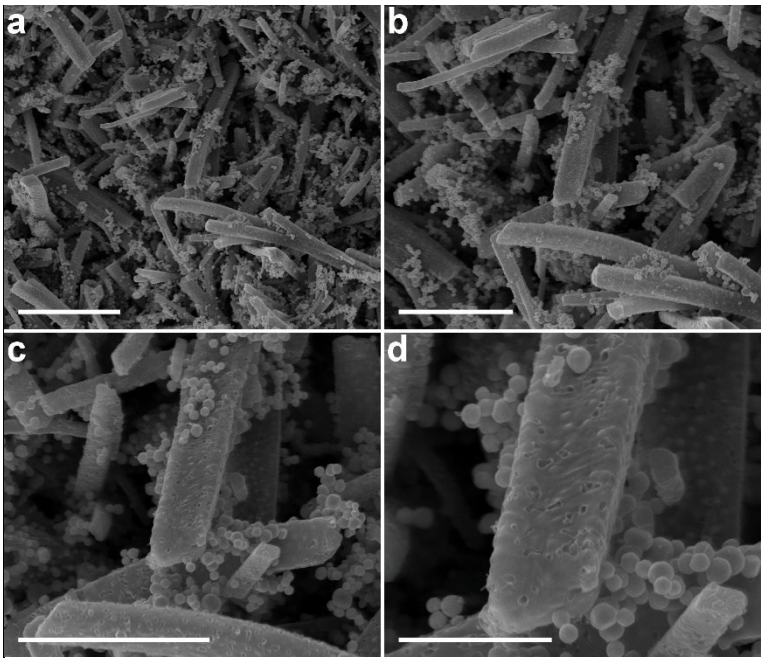

Figure S4. SEM images of Cu-C at different magnification. Scale bars: (**a**) 10 μm; (**b**, **c**) 5 μm; (**d**) 2 μm.

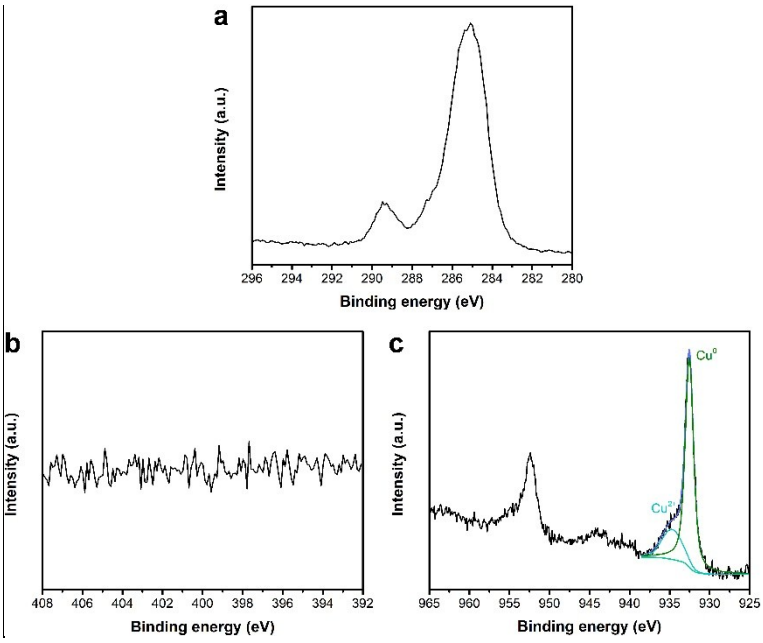

Figure S5. XPS survey spectra of Cu-C: (**a**) C 1s; (**b**) N 1s; (**c**) Cu 2p.

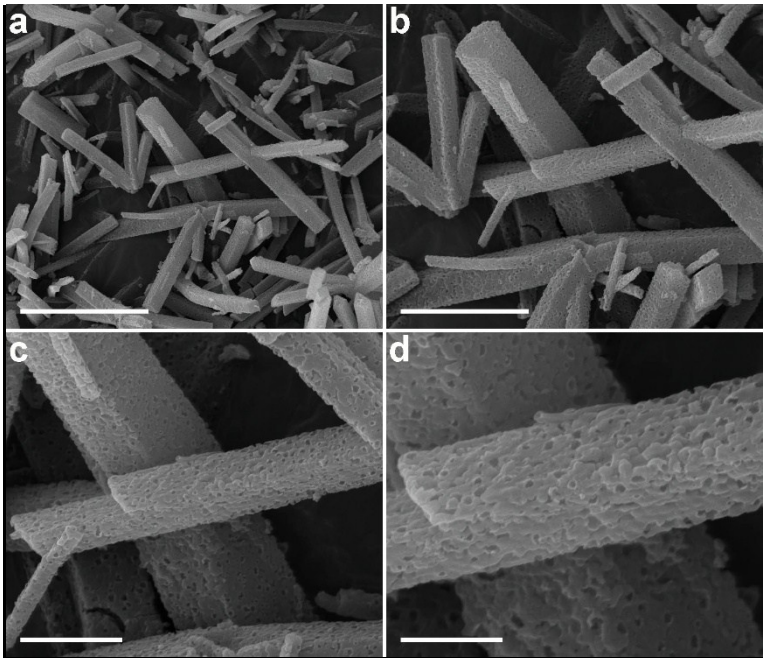

Figure S6. SEM images of Cu-C-AF at different magnification. Scale bars: (**a**) 10 μm; (**b**) 5 μm; (**c**) 2 μm; (**d**) 1μm.

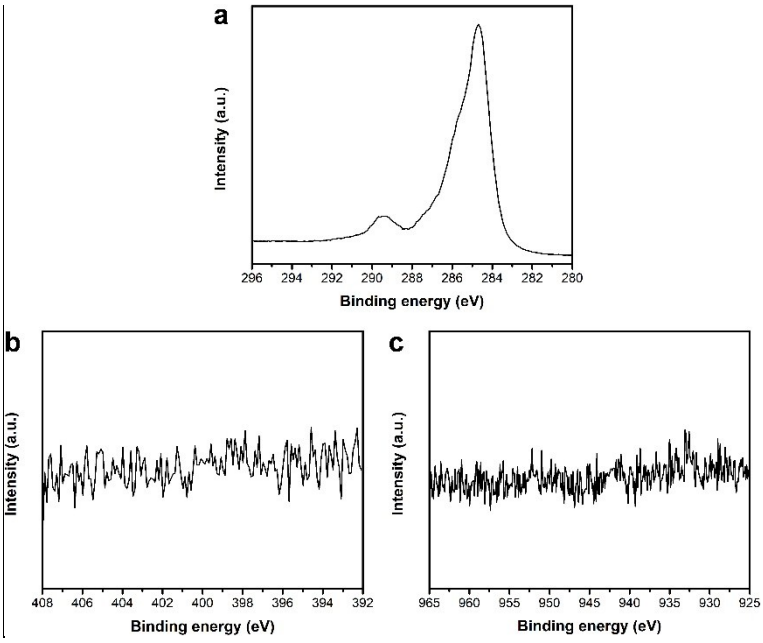

Figure S7. XPS survey spectra of Cu-C-AF: (**a**) C 1s, (**b**) N 1s, (**c**) Cu 2p.

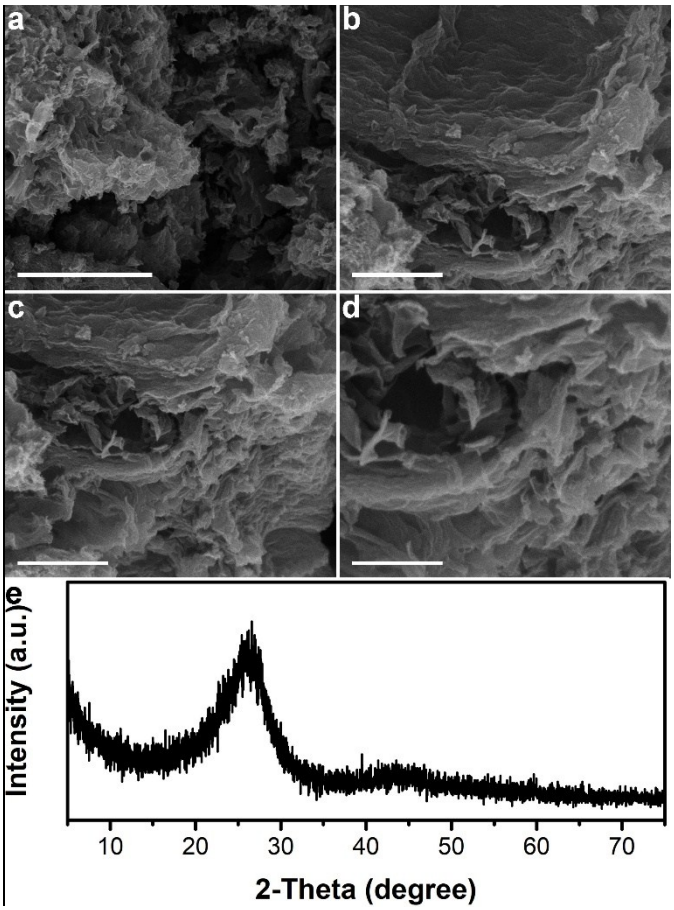

Figure S8. SEM images of N-C at different magnification. Scale bars: (**a**) 3 μm; (**b**) 1 μm; (**c**) 1 μm; (**d**) 0.5 μm. (**e**) XRD pattern of N-C.

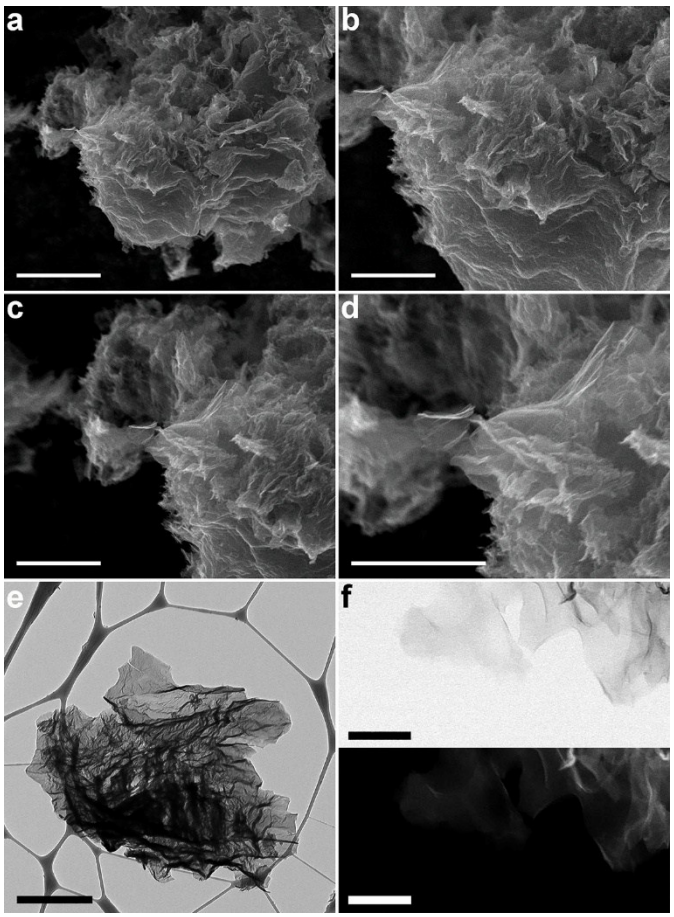

Figure S9. SEM images of Cu-N-C at different magnification. Scale bars: (**a**) 5 μm, (**b**) 2.5 μm, (**c**) 2.5 μm, (**d**) 2 μm. TEM images of Cu-N-C at different magnification. Scale bars (**e**) 2 μm; (**f**) 200 nm (top-bright field image, bottom-dark field image).

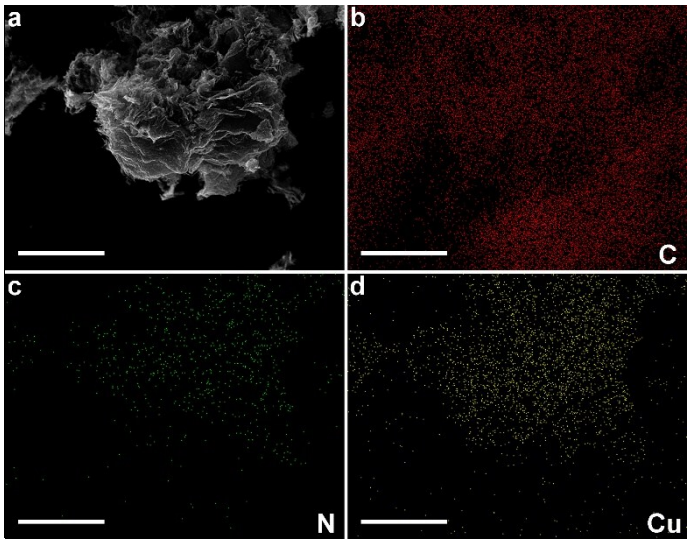

Figure S10. EDS elemental mapping images of Cu-N-C: (**a**) SEM image, (**b**) carbon, (**c**) nitrogen, (**d**) copper. Scale bars: 10 μm.

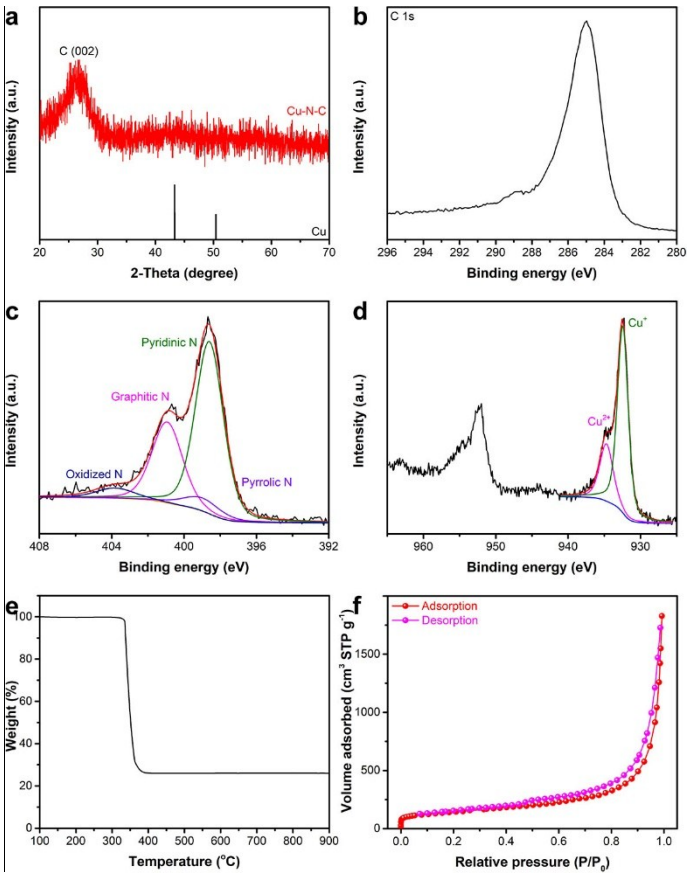

Figure S11. (**a**) XRD pattern of Cu-N-C and Cu (JCPDF: No. 04-0836). (**b, c, d**) High resolution XPS spectra of C 1s, N 1s and Cu 2p for Cu-N-C, respectively. (**e**) TGA thermogram of Cu-N-C under air atmosphere with a ramping rate of 10 °C min^{-1}. (**f**) Nitrogen adsorption/desorption isotherms of Cu-N-C.

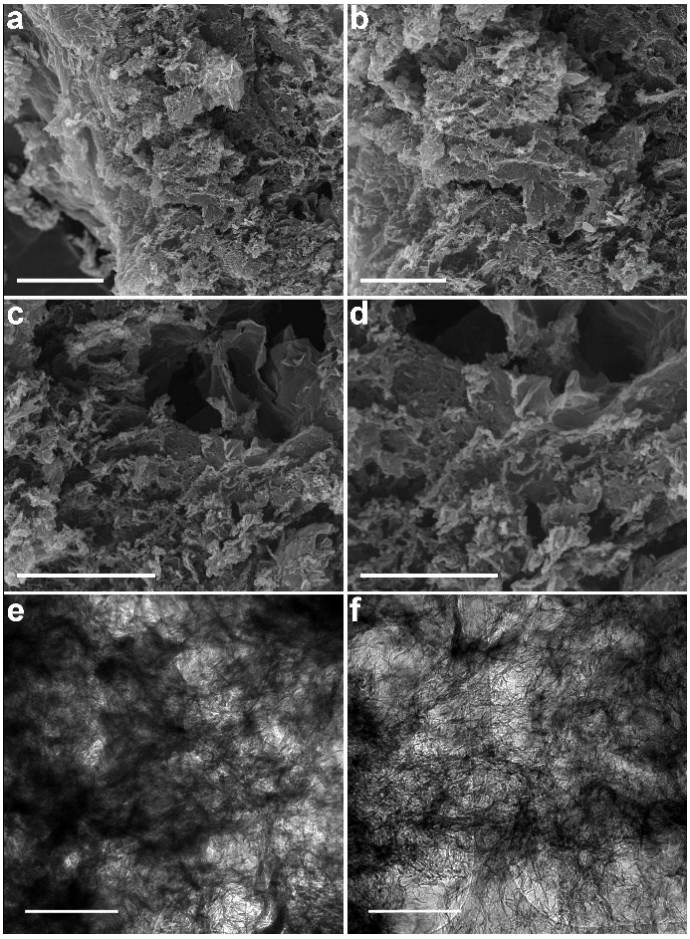

Figure S12. SEM images of Cu-N-C-BF at different magnification. Scale bars: (**a**) 5 μm, (**b**) 2.5 μm, (**c**) 2 μm, (**d**) 1 μm. (**e, f**) TEM images of Cu-N-C-BF. Scale bars: 200 nm.

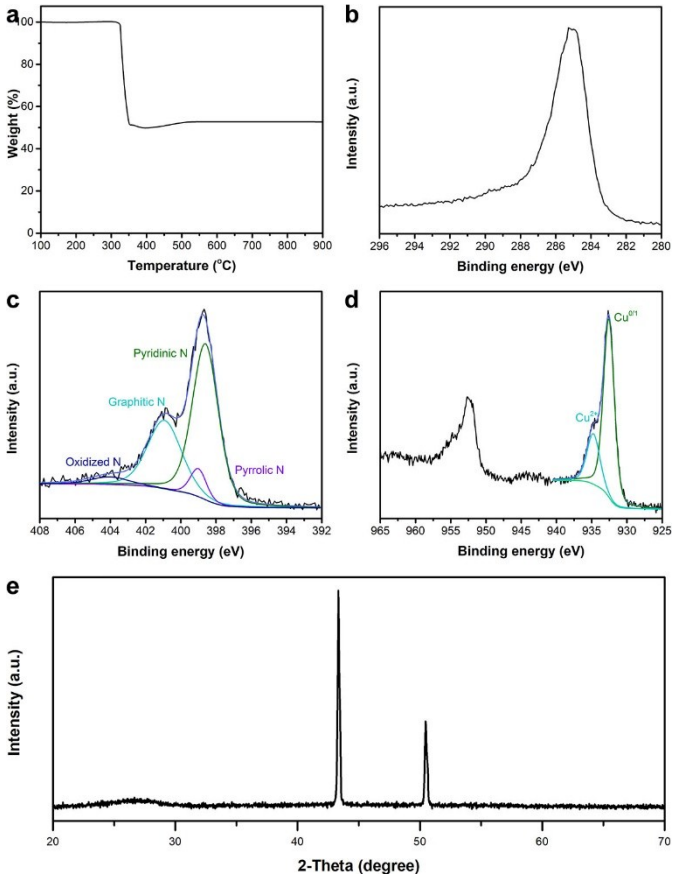

Figure S13. (**a**) TGA thermogram of Cu-N-C-BF under air atmosphere with a ramping rate of 10 °C min^{-1}. XPS survey spectra of Cu-N-C-BF (**b**) C 1s, (**c**) N 1s, (**d**) Cu 2p. (**e**) XRD pattern of Cu-N-C-BF. The two sharp peaks belong to the cubic metal Cu (JCPDF: No. 04-0836). The broad peak at around 26.5° can be attributed to graphic carbon.

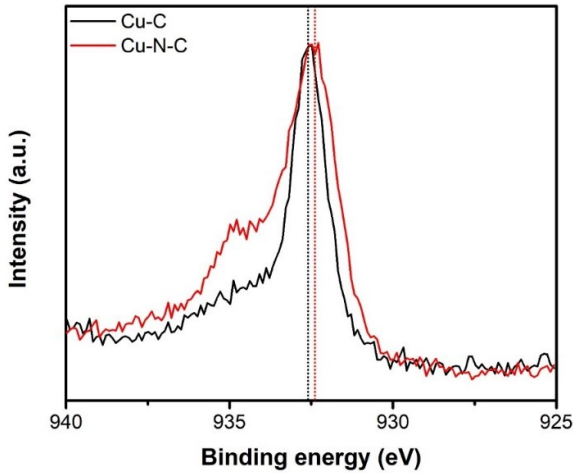

Figure S14. XPS Cu 2p profiles of Cu-C and Cu-N-C. Compared with Cu^0 in Cu-C, Cu^+ in Cu-NC shows a little redshift.

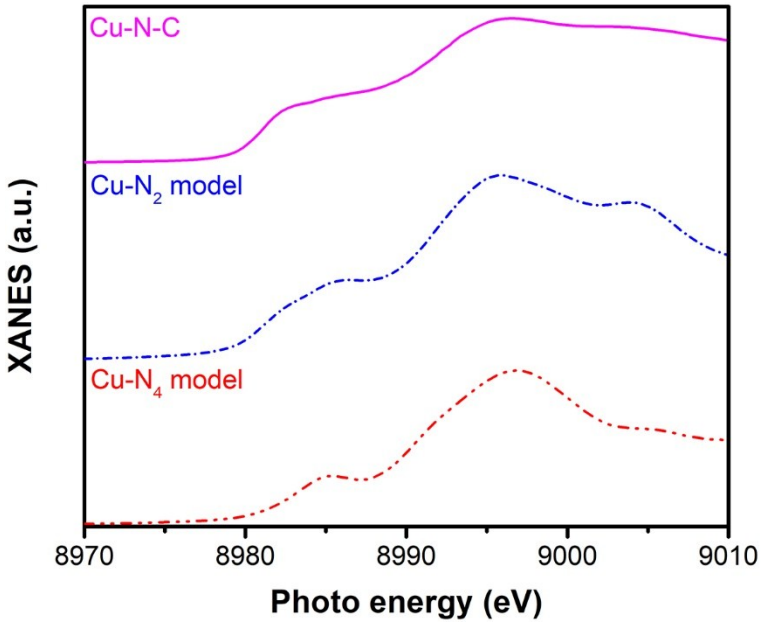

Figure S15. Cu K-edge XANES experimental spectrum for Cu-N-C (pink), and the calculated spectra for the proposed $Cu\text{-}N_2$ (blue) and $Cu\text{-}N_4$ (red) model structures.

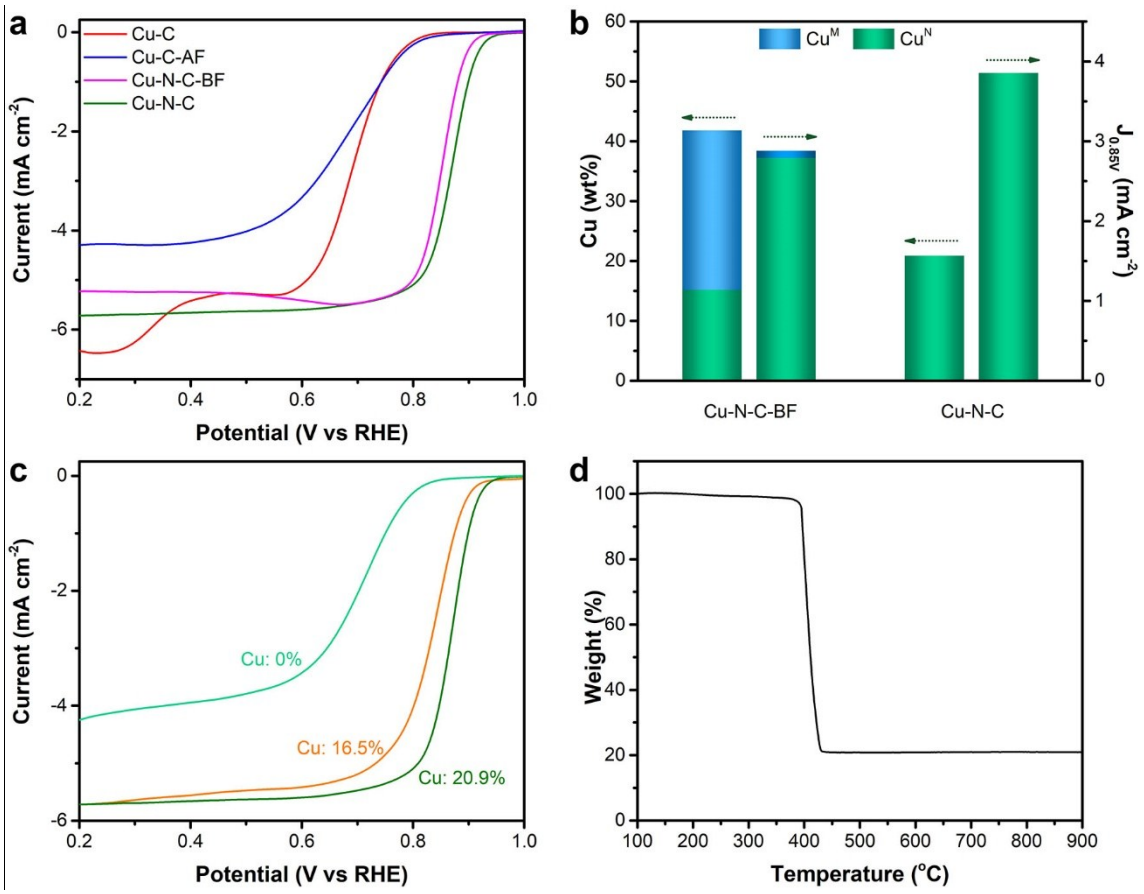

Figure S16. (**a**) Polarization curves Cu-C, Cu-C-AF, Cu-N-C-BF and Cu-N-C catalysts in 0.1 M aq. KOH solution (oxygen saturated). Rotation speed: 1600 r.p.m.; scan rate: 5 mV s^{-1}. (**b**) Compositions of metallic Cu (Cu^M) and coordinated Cu (Cu^N) in Cu-N-C-BF and Cu-N-C, as well as their contributions to the polarization current at 0.85 V, respectively. (**c**) Polarization curves Cu-N-C catalysts with different Cu contents in 0.1 M aq. KOH solution (oxygen saturated). Rotation speed: 1600 r.p.m.; scan rate: 5 mV s^{-1}. (**d**) TGA thermogram of Cu-N-C (weight ratio of the precursor and dicyandiamide, 1:5) under air atmosphere with a ramping rate of 10 °C min^{-1}.

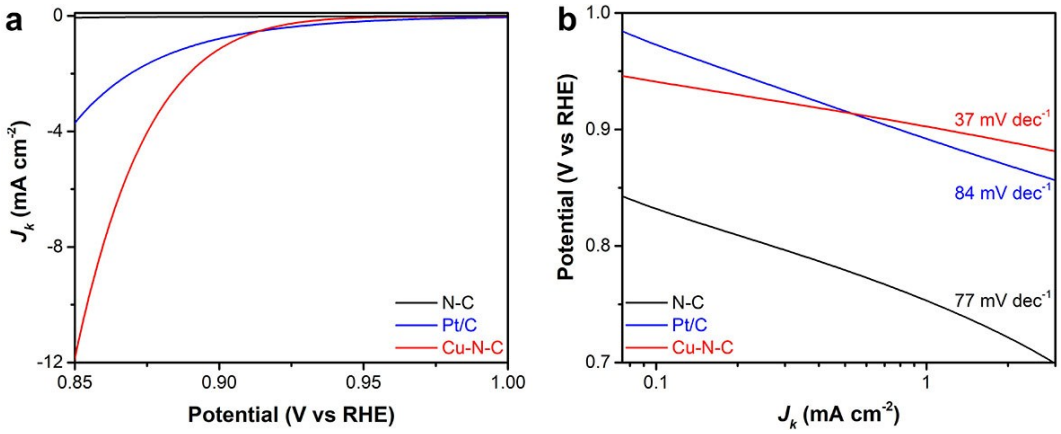

Figure S17. (**a**) Kinetic current-potential dependence curves for Cu-N-C, N-C and Pt/C catalysts in 0.1 M aq. KOH solution (oxygen saturated). (**b**) Corresponding Tafel plots obtained from (**a**).

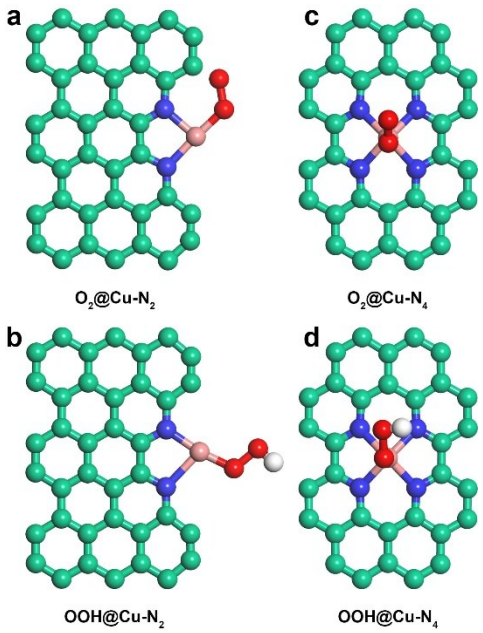

Figure S18. (**a**, **b**) O_2 and OOH adsorption configuration on Cu-N_2, respectively. (**c**, **d**) O_2 and OOH adsorption configuration on Cu-N_4, respectively. Green, blue, light pink, red and white ivory balls represent carbon, nitrogen, copper, oxygen and hydrogen atoms, respectively.

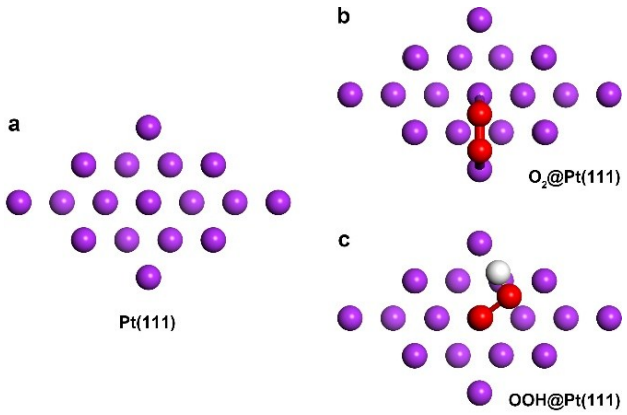

Figure S19. (**a**) Optimized structure of Pt(111). (**b**, **c**) O_2 and OOH adsorption configurations on Pt(111). Purple, red and white ivory balls represent platinum, oxygen and hydrogen atoms, respectively.

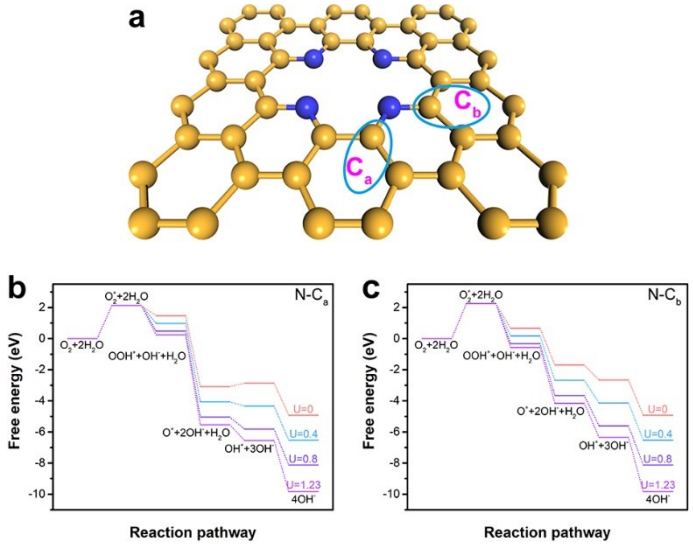

Figure S20. (**a**) Optimized structure of N-C. (**b**, **c**) Free energy diagrams of ORR reaction pathways on N-C_a and N-C_b at different overpotential U (V), respectively. Yellow and blue ivory balls represent carbon and nitrogen atoms, respectively.

Table S1. Structural parameters extracted from the EXAFS fitting

Sample	Path	N[a]	R (Å)[b]	σ^2 (10^{-3}Å^2)[c]	ΔE_0 (eV)[d]	R factor
Cu-N-C	Cu-N	2	2.00	4.9	1.8	0.008
	Cu-N	4	1.86	7.3		

[a] Coordination number; [b] Bonding distance; [c] Debye-Waller factor; [d] Energy shift.

Table S2. Cu contents in various catalysts determined by ICP-OES and TGA

Content	Cu-N-C-BF	Cu-N-C	Cu-N-C (1:5)
ICP-OES (wt %)	41.8	20.9	16.5
TGA (wt %)	42.1	21.3	16.7

Table S3. ORR parameters for recently reported non-precious metal based catalysts in alkaline electrolyte

Catalyst	Electrolyte	$E_{1/2}$ (V vs RHE)	Tafel slope (mV dec^{-1})	Reference
Cu-N-C	0.1 M KOH	0.869	37	This work
Co_3O_4/N-rmGO	0.1 M KOH	0.83	42	Nat. Mater. 2011, 10, 780.
Co_3O_4/rmGO	0.1 M KOH	0.79	50	Nat. Mater. 2011, 10, 780.
FePhen@MOF-$ArNH_3$	0.1 M KOH	0.86	--	Nat. Commun. 2015, 6, 7343.
N-CG–CoO	0.1 M KOH	0.81	48	Energy Environ. Sci. 2014, 7(2): 609-616.
$Co_{0.50}Mo_{0.50}O_yN_z$/C	0.1 M KOH	0.76	71	Angew. Chem. Int. Ed. 2013, 52(41): 10753-10757.
Fe–N/C–800	0.1 M KOH	0.81	--	J. Am. Chem. Soc. 2014, 136, 11027-11033.
rGO-$Cu_{2-x}S$	0.1 M KOH	0.82	67	ACS Catal. 2015, 5, 2534−2540
Fe-N-CNFs	0.1 M KOH	0.82	--	Angew. Chem. Int. Ed. 2015, 54, 8179-8183.
S,N-Fe/N/C-CNT	0.1 M KOH	0.85	--	Angew. Chem. Int. Ed. 2017, 56, 610 – 614
Fe_3C@N-CNT	0.1 M KOH	0.85	78	Energy Environ. Sci., 2016, 9, 3092 –3096

Table S4. Adsorption energies of O_2 and OOH and structural parameters on Cu-N_2, Cu-N_4 and Pt(111)

Structure	O_2 (eV)	OOH (eV)	O-O (Å, O_2)	O-O (Å, OOH)
Cu-N_2	−2.12	−2.01	1.455	1.460
Cu-N_4	0.74	−0.23	1.289	1.435
Pt(111)	−0.34	−0.83	1.361	1.426

Adsorption energies are calculated by $E_{ads} = E_{product} - E_{reactant}$.